



Cite this: *Environ. Sci.: Water Res. Technol.*, 2024, 10, 263

Particle and DBP removal efficiency and toxicity evaluation of polypropylene cotton filters in household drinking water purification systems†

Linlin Pan,^{ab} Yuan Zhuang,^{*b} Ruya Chen,^{bd} Yitian He^{bc} and Baoyou Shi ^{*bc}

Polypropylene cotton filters (PCFs) are traditionally considered an essential pretreatment unit for coarse-particle removal in household water purification systems. However, the actual roles of PCFs in controlling drinking water quality risks, especially in discolored water, have not been well understood, and the particulate matter collected on PCFs has not been well-studied. In this study, the detailed characterization of a used PCF found that many types of iron particles, which usually are dominant in drinking water distribution systems, including magnetite, hematite, maghemite, goethite, and lepidocrocite, were mainly captured by the outer-most layer (20% of the total thickness) of PCF. MTT tests using human hepatocytes showed that the iron particles captured by the PCF exhibited obvious cytotoxicity, and the particle toxicity decreased from the outer layer to the inner layer, indicating that PCFs can efficiently reduce iron-particle-associated toxicity risk. In addition, the PCF had a significant ability for the enrichment of trace organic pollutants (e.g. perfluorooctanoic acid), which would further reduce the water quality risks. Furthermore, some common opportunistic microbial pathogen species, including *Acinetobacter*, *Mycobacteria*, and *Pseudomonas*, could be intercepted effectively by the PCF. Filtration experiments using a new PCF showed that PCF was effective not only in particle removal (96.1–99.8%) but also in disinfection by-product (DBP) removal (7.9–65.9%). Above all, as a household water treatment unit, PCFs not only protect the purification units but can also have many previously unrecognized functions in water quality risk control.

Received 20th August 2023,
Accepted 28th October 2023

DOI: 10.1039/d3ew00615h

rsc.li/es-water

Water impact

Polypropylene cotton filters (PCFs) are traditionally considered an essential pretreatment unit for coarse particle removal in household water purification systems. However, the actual roles played by PCFs in controlling drinking water quality risks, especially in discolored water, have not been well understood, and the particulate matter enriched on PCFs has not been well-studied. In this study, the detailed characterization of a used PCF demonstrated that many kinds of iron particles, which usually are dominant in drinking water distribution systems, including magnetite, hematite, maghemite, goethite, and lepidocrocite, were mainly captured by the most outer layer (20% of the total thickness) of PCF. MTT tests performed using human hepatocytes showed that the iron particles captured by the PCF exhibited obvious cytotoxicity, and the particle toxicity decreased from the outer layer to the inner layer, indicating that the PCF can efficiently reduce iron-particle-associated toxicity risks. Metal oxides, especially iron oxides, found in the PCF can interact with the DNA and nuclear proteins, thereby triggering DNA damage and eventually leading to human hepatocyte apoptosis. Overall, the PCF is still a reliable tap water purification unit.

1. Introduction

Drinking water distribution systems (DWDS) are receiving increasing attention in the process of drinking water purification and distribution process. The transportation process through DWDS often deteriorates water quality, even to the extent of quality violations to occur. Although it is often assumed that bacteria are more detrimental to the human body, iron-based particles from DWDS have been shown to be toxic to human hepatocytes.¹ Under hydraulic disturbance, the loose iron deposits in DWDS generate discoloration, and the particles may be consumed by the users *via* drinking. The loose deposits in DWDS have been shown to pose health risks in several

^a School of Municipal and Environmental Engineering, Shandong Jianzhu University, Jinan 250101, P R China

^b Key Laboratory of Drinking Water Science and Technology, Research Center for Eco-Environmental Sciences, Chinese Academy of Sciences, Beijing 100085, China. E-mail: yuanzhuang@rcees.ac.cn, byshi@rcees.ac.cn

^c University of Chinese Academy of Sciences, Beijing 100049, China

^d School of Environmental Science and Engineering, Zhejiang Gongshang University, Hangzhou, 310012, Zhejiang, China

† Electronic supplementary information (ESI) available. See DOI: <https://doi.org/10.1039/d3ew00615h>



2.4 Discolored water treatment by the new and used PCFs

To evaluate the efficiency of the PCFs in treating discolored water, three faucets (faucets 1#, 2# and 3#) were established at the same ends of the DWDS in our laboratory. A 50 cm galvanized steel pipe with serious corrosion, which had been used for more than 20 years, was placed in the front section of the three taps (Fig. S2†) to ensure that the water discoloration phenomenon would often occur. These faucets had a 50 mL min⁻¹ flow rate limit and were accessible continuously throughout the day. Faucet 2# was connected to the used PCF and faucet 3# was connected to the new PCF. When tap water from faucet 1# became discolored, water from faucet 1# was used as the sample before PCF treatment, while the water samples from faucets 2# and 3# were designated as samples after treatment by the new and used PCFs, respectively. Disinfection by-products (DBPs) and metal ions in the collected water before and after treatment were analyzed.

2.5 Characterization

The morphologies of particles in all PCF samples were characterized using transmission electron microscopy (TEM, FEI, Tecnai G2 F20), X-ray diffraction (XRD, X'Pert 3 Powder), and X-ray fluorescence (XRF, ARL Perform'X 4200). An Agilent 1200 HPLC system was used in conjunction with an Agilent 6460 Triple Quadrupole (QQQ) mass spectrometer (Agilent Technologies, USA) in the negative electrospray ionization (ESI⁻) mode to analyze PFOA concentration. Pretreatment of the water samples was done using established procedures within a few weeks.¹⁸ DBPs are generated through chemical reactions between disinfectants (such as chlorine, chloramine, or ozone) and organic or inorganic matter present in the water being treated. The common DBPs in drinking water are some organic compounds. The residual chlorine concentration in the sampling area ranged from 0.1 to 0.5 mg L⁻¹. The following DBPs were analyzed: a trihalomethane (THMs), namely trichloromethane (TCM), a haloacetonitrile (HANs), namely dichloroacetonitrile (DCAN), and haloacetic acids (HAAs), including dichloroacetic acid (DCAA) and trichloroacetic acid (TCAA). The water samples were filtered through 0.45 μm membrane filters before being tested for DBPs. Based on the USEPA Standard Methods 551.1 and 552.3, the C-DBPs and N-DBPs analysis was done using an Agilent 7890 gas chromatograph with an electron capture detector (GC/ECD).¹⁹ The column used was an HP-5 fused silica capillary column (30 m, 0.25 mm I.D. with 0.25 μm film thickness).²⁰

The details of other analysis methods, including DNA extraction and quantitative polymerase chain reaction (qPCR), and statistical analysis are shown in ESI†

2.6 Water quality analysis

Temperature, pH, free chlorine, dissolved oxygen (DO), and turbidity were measured at the moment of collection. A portable water quality testing device was used to measure temperature, DO, and pH. (HD40Q, Hach, USA). The USEPA

DPD technique was used to quantify free chlorine (DR300, Hach, USA).

For metal ion detection, we divided the two-centimeter-thick PCF into three layers from the inside to the outside and cut it into 2 mm thick blocks measuring one centimeter by one centimeter. They were then placed in a sterile centrifuge tube and pulsed with ultrapure water using ultrasound for 60 minutes to yield three water samples. These three samples and the water samples before and after filtration were tested for metal concentration. A 50 mL polypropylene centrifuge tube was used to collect water for total and soluble metal concentration analysis. One aliquot of each water sample was digested using 1% (w/w) HNO₃ for 24 h to analyze the concentration of total metals.²¹ The other aliquot of water sample was filtered through a 0.22 μm polyethersulfone membrane to analyze the concentration of soluble metals. Inductively coupled plasma mass spectrometry (ICP-MS, NexION 300X 0–200 g L⁻¹) was used to analyze the metal concentrations. Inductively coupled plasma optical emission spectroscopy (ICP-OES, OPTIMA 8300 0.2–200 mg L⁻¹) was used to determine the amounts of individual metallic elements in the water samples. Fe, V, Zn, Al, Cr, Mn, Sr, Ba, and Cu were among the elements analyzed. The total quantity of particles was verified by a Desktop Laser Particle Analyzer GR-1500A produced by Hangzhou Grean Technology Co., Ltd. It could detect particles with a particle size of more than 1 μm. For quality control, standard samples with established concentrations were utilized. The ESI† section contains other details regarding analysis and testing.

2.7 Statistical analysis

For quality filtering, QIIME (version 1.17) was employed with the following criteria: (i) the 300 bp reads were trimmed at any site with an average quality score of 20 or above across a 50 bp sliding window, while truncated reads less than 50 bp were discarded. (ii) Reads with unclear characters, precise barcode matching, and two nucleotide mismatches in primer matching were all eliminated. (iii) Only sequences with overlaps greater than 10 bp were constructed in the order in which they overlapped. The reads that could not be put together were discarded. Sequences with 97 percent similarity were clustered into operational units (OTUs) using UPARSE (version 7.1; <http://drive5.com/uparse/>), and chimeric sequences were identified and removed using UCHIME. With a confidence level of 70%, all sequences were assigned to taxonomic ranks using the RDP Classifier (<http://rdp.cme.msu.edu/>) against the silva (SSU115) 16S rRNA database.

All statistical analyses were performed using the vegan package in R (v.4.0.2; <http://www.r-project.org/>).²² A bar chart (phylum and class level) and a heatmap were used to depict the makeup of the bacterial community (genus level). The alpha-diversity (Shannon index) in the DWDS bacterial community was calculated using Mothur calculations (version v.1.30.1 http://www.mothur.org/wiki/Schloss_SOP#Alpha_diversity) and Student's *t*-test. To reveal the



variance among the microbial community compositions with spatiotemporal fluctuations in the DWDSs, principal coordinate analysis (PCoA) and analysis of similarity (ANOSIM) based on the Bray–Curtis distance were used. The Bray–Curtis distance was utilized to explain the change in microbial community compositions owing to physicochemical conditions using permutational multivariate analysis of variance (PERMANOVA).²³ To represent the difference in dominant species among the samples, the Kruskal–Wallis *H* test was utilized. For convenient plots, gene copy numbers were $\log(x + 1)$ transformed, where *x* is the gene copy number quantified by qPCR.²⁴

3. Results and discussion

3.1 Characteristics of particle removal by PCF

In the old used PCF, a layered structure with obvious color changes was observed (Fig. 1a). The outer layer (0.4 cm) showed a brown color, while the intermediate layer (0.4 cm) and the inner layer (1.2 cm) were orange and yellow (Fig. 1b). The contents of each layer of the new PCF and the used PCF were examined by XRD to better understand the crystal form of the substances enriched on

each layer of the PCFs. The XRD (Fig. 1c) analysis revealed the presence of goethite, quartz, hematite, maghemite, akaganeite, lepidocrocite, and magnetite, and in the outer layer of the PCF, goethite exhibited the greatest composition at 27%, followed by quartz at 23% (Fig. 1d). These elements resemble the primary components of the pipe scale described in the previous studies.^{1,25} Iron is the major component of the corrosive pipe scale, and it enters the water with water quality fluctuations, resulting in discoloration and eventually reaching the consumers.²⁶ Based on the XRD results, these oxides were mainly concentrated in the outer layer of the PCFs. The XRD results of the intermediate layer and the inner layer were similar to the new PP cotton, indicating that only few crystals were enriched in the intermediate layer and the inner layer.

The percentages of iron oxides in the three layers of the used PCF sample from outside to inside were 11.2%, 4%, and 2.4%, respectively, according to the XRF analysis results in Fig. 2, which further indicates that the particles were mainly captured by the outer layer of the PCF. This is in accordance with the XRD result that these oxides were mainly detected in the outer layer. Iron occupied the highest percentage among

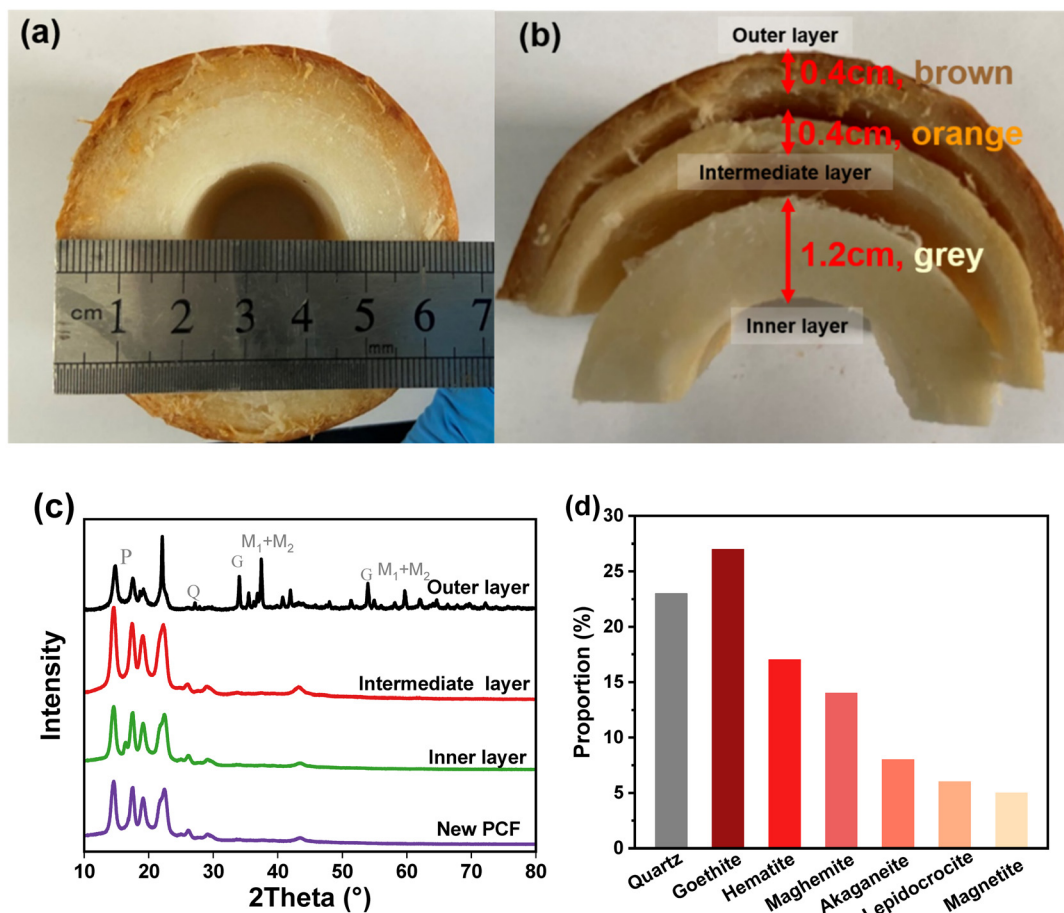


Fig. 1 (a) Cross-section photograph of the PCF, (b) photograph of different layers of the PCF, (c) XRD analysis of the used PCF and new PCF (G: goethite, Q: quartz, P: polypropylene, M₁: maghemite, M₂: magnetite), and (d) proportion of metal oxides in the PCF.



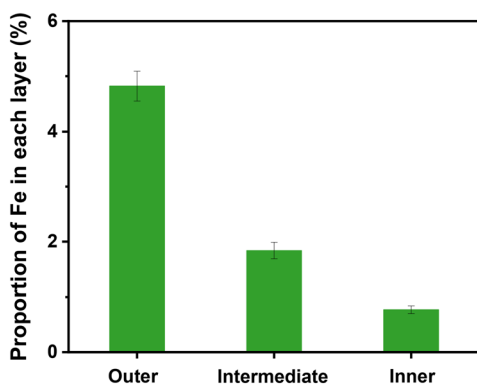


Fig. 2 XRF analysis of Fe content in the three layers (outer layer, intermediate layer, and inner layer) of the used PCF.

the elements in each layer, followed by silicon, which is also consistent with the XRD results. In the outer and intermediate layers, iron contributed to more than 40% of the total content. The principal components of the sediments enriched on the PCF, according to XRD and XRF analysis, were different kinds of iron oxides, consistent with the components of loose deposits obtained from DWDS reported in previous research^{27–30} and indicating the effective removal of particles from DWDS by the PCF. Fig. 3 shows the SEM images of particles on the outer layer of the PCF, and the presence of urchin-like nanorods similar to FeOOH morphology was found,^{1,6} which is in accordance with the XRD and XRF observations. The sharp surface of the particles may enhance their potential to damage cells and hence their toxicity risks.^{1,31}

3.2 Particle-associated toxicity risk control by PCFs

Iron nanoparticles can quickly accumulate in the liver and spleen as a result of macrophage phagocytosis and trapping; even when iron oxide nanoparticles are tailored to target specific tissues or organs, liver absorption has been shown to be the most effective clearance route.^{1,32} Humans are more likely to be exposed to iron particles through drinking water. Healthy human liver cells were selected to assess the toxicity of the particles from different layers of the PCF. Fig. S3† shows the fluorescence microscopy images of the cells before and after treatment with the particle samples; the green cells are alive and the red cells are dead. After 72 hours, no dead cells were found in the blank sample (without particles). After treatment with the particles from three layers of the PCF, dead cells appeared in all the samples after 72 hours. The cell viability of the samples treated with particles from the different layers of PCF followed the order: outer layer < intermediate layer < inner layer (Fig. 4), which indicates that the particles intercepted by the outer layer of the PCF had the highest toxicity. Thus, the PCF, especially the outer layer, is effective in reducing the toxicity risks induced by the particles. It has been discovered that iron oxides interact with the DNA and nuclear proteins, thereby triggering DNA damage and eventually leading to cell cycle regulation, apoptosis or cancer.^{33,34} Iron oxides may not only take electrons directly from the DNA but also use DNA as an electron donor to make reactive oxygen species from oxygen, which would dramatically accelerate oxidative damage to cells.¹

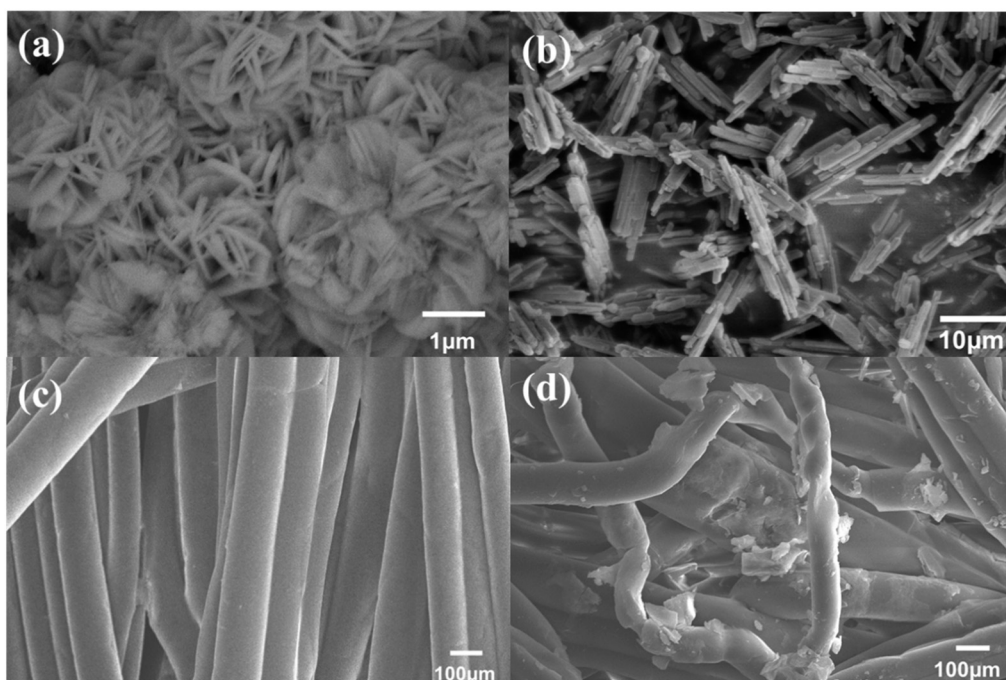


Fig. 3 SEM images of (a and b) particles on the outer layer of PCF, (c) new PCF, and (d) used PCF.



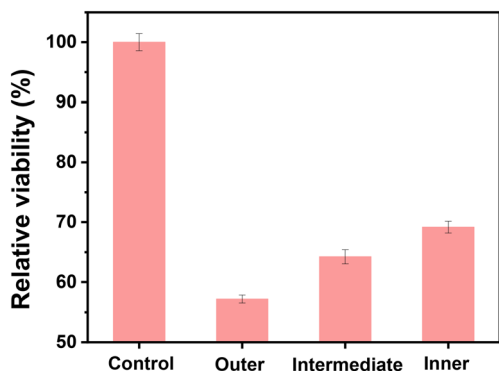


Fig. 4 Relative viabilities determined via the MTT assay of liver cells with the particles from the three layers (outer layer, intermediate layer, and inner layer) of the used PCF.

Among the particles obtained from the DWDS, besides the cytotoxicity originating from the metal oxide components, the particles might have further toxicity risks due to organic matter accumulation.³⁵ A series of perfluorooctanoic acid (PFOA) solutions with initial concentrations (1, 10, 20, 50, and 100 $\mu\text{g L}^{-1}$) were used to evaluate the pollutant accumulation ability of the particles from the outer layer of PCF (Fig. S4†). The PFOA accumulation efficiency of the particles under different concentrations were 51.52%, 25.06%, 16.71%, 10.63%, and 8.43%, respectively. The Langmuir model and the Freundlich model (eqn (S1) and (S2)†) were applied to evaluate the most suitable adsorption isotherm for PFOA adsorption onto the particles (Fig. S5†).^{36,37} The R^2 values of the Langmuir model and Freundlich model were 0.991 and 0.994, indicating that the adsorption process was fitted well by the both models. The maximum adsorption capacity was 0.123 mg g^{-1} , which indicates the strong PFOA accumulation ability of the particles on the PCF. Thus, PCFs can further reduce the toxicity risks induced by toxic organics, such as PFOA, through particle accumulation.

3.3 Bacterial community composition characteristics of PCF

The PCF had 321 different OTUs, 100 of which were shared among the three layers (Fig. 5b). Interestingly, though the particles mainly accumulated in the outer layer, the microorganism diversity was found to be higher in the inner layer: 108 OTUs existed in the inner layer, which was sharply higher than the other layers. The average number of gene copies in the PCF decreased from outside to inside, and the average number of water samples before filtration was much higher than that after filtration (Fig. 5a). The PCF had a certain microorganism filtering ability. In the intermediate and inner layers, *Actinobacteriota* was the most abundant phylum, while *Proteobacteria* was the most dominant in the outer layer (Fig. S6†), indicating the higher chlorine-resistance ability of *Proteobacteria* as the outer layer would come in contact with more chlorine. *Actinobacteriota* was also the most abundant class (Fig. S6†). The PCF had a high proportion of four genera, including *Rhodococcus*, *Phreatobacter*, *Sphingomonas*, and *Delftia* (Fig. S6†). The four genera constituted 92.98%, 96.68%, and 95.99% of the bacteria in the outer, intermediate and inner layers, respectively. The most abundant genus in the three layers of the PCF was *Rhodococcus*, accounting for 46.60%, 71.43%, and 72.65% of bacteria in the outer, intermediate and inner layers, respectively. In recent years, *Phreatobacter* has been found to be a prevalent genus in DWDS,^{38–41} and it was also the most prevalent in juvenile biofilms formed in chlorine-disinfected drinking water samples of (within 3 months).³⁸ Similarly, *Phreatobacter* was the second-highest abundant genus in the outer layer, and its prevalence was much higher than that in the intermediate and inner layers. Thus, the outer layer had less bacteria than the inner layer due to more contact with chlorine. *Sphingomonas* is a common genus in DWDS biofilms and exists constantly and consistently in the biofilms studied across different times and conditions.^{42,43} It has been pointed out that the relative abundance of *Actinomycetes* positively correlates with total chlorine.³⁹ This might be the reason that the inner layer had the highest diversity.



Fig. 5 (a) Quantitative analysis of 16S rRNA for total bacteria of three layers and the water samples treated by PCF (B-PCF: before treatment by PCF; A-PCF: after treatment by PCF), (b) Venn graph of detected taxa of three layers (outer layer, intermediate layer, and the inner layer) of used PCF.



Pathogens have been detected in biofilms growing in DWDS and represent substantial risks to human health.^{4,39,44} Some opportunistic pathogens can thrive in water with 2 mg L⁻¹ chloramine.⁴⁵ Several species of *Acinetobacter*, *Mycobacteria*, and *Pseudomonas*^{4,28,46,47} that are common opportunistic pathogens were detected in this study (Table S2†). At the OTU level, there were 108 distinct populations in the inner layer, which included *Pseudomonas*. Further, 22 and 13 endemic populations were found in the intermediate layer and the outer layer, respectively. The relative abundance of these three genera decreased from outside to inside. The residual chlorine decreased from 0.65 mg L⁻¹ to 0.40 mg L⁻¹ when the tap water was filtered by the PCF, which may also be the explanation for the greater microbial abundance in the inner layer. Meanwhile, *Pseudomonas* has also been found in 0.5 mg L⁻¹ chlorine water,⁴⁸ which might also be the reason for its existence in the inner layer. Therefore, the microbial risks were still limited due to the low quantity of biomass in the inner layer.

3.4 DBP removal by PCF from discolored water

The efficiency of PCF in treating discolored water was evaluated. DBP levels are important water quality indexes related to toxicity in DWDS.^{49,50} The removal rates of TCM, DCAN, DCAA, and TCAA by the used PCF were 20.8%, 10.8%, 24.7%, and 21.8%, respectively (Fig. 6). Correspondingly, the removal rates of TCM, DCAN, DCAA, and TCAA by the new PCF were 65.9%, 12.1%, 28.7%, and 7.9% respectively. Surprisingly, the PCF had a certain DBP removal effect. Overall, the DBP removal effectiveness of the used PCF was lower than that of the new PCF. In addition to TCAA, the new PCF had a better DBP treatment capability. A decrease in the removal of THMs and HAAs by POU filters with time or facility aging has also been reported in the literature,⁵¹ but the reason is yet to be further studied.

DBPs are directly proportional to the humic acid content.^{52,53} The natural organic matter (NOM) enrichment value of the outer layer of the PCF was found to be the highest (Fig. 7 and S8†), and those of the intermediate and inner layers were less, which indicates that the particles in the outer layer may help accumulate NOM. The water had a

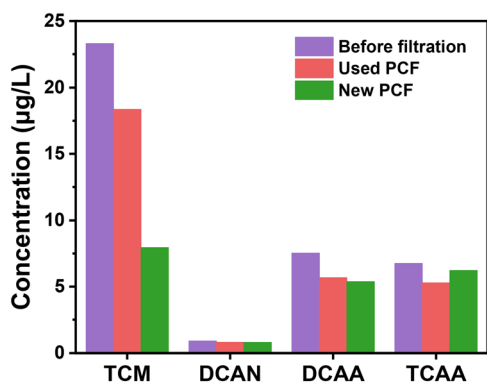


Fig. 6 DBPs changes in water treated by the new and used PCFs.

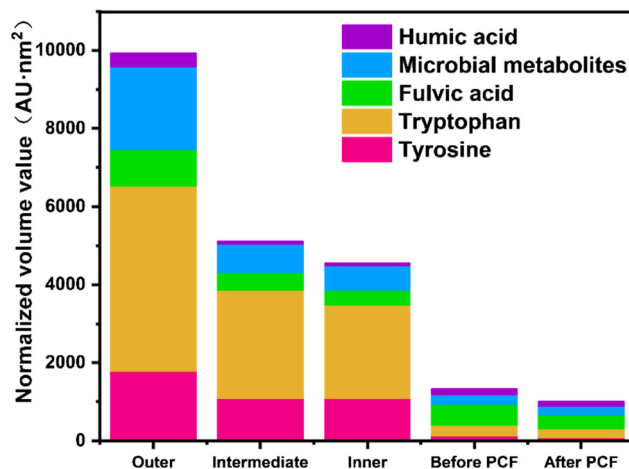


Fig. 7 Integration of the EEMs on each layer of the PCF, and the change in EEM concentration before and after filtration with the PCF.

lower content of NOM after filtration by the PCF, further proving that NOM was intercepted by the PCF. The presence of NOM in the PCF might be an important reason for the low DBP removal efficiency of the old PCF.

When discoloration happens, it is necessary to consider the efficiency of the PCF element in intercepting particles. Metal concentrations in the discolored water before and after filtration by the PCF are shown in Fig. S7.† The concentrations of iron, aluminum, and manganese were high, and certain hazardous elements, such as lead and arsenic, were also found to exist, which is comparable to the dominant metal composition of particles previously reported in DWDS.^{26,29,38} The dominant components in the discolored water were also very comparable to the metal components captured by the PCF. Furthermore, the concentrations of lead and arsenic in the discolored water were 5.23 µg L⁻¹ and 63.9 µg L⁻¹, respectively. In addition to metal strontium and metal barium, PCF had a 96.1% to 99.8% interception efficiency toward other metals, which was comparable to that of the new PCF (96.7%) (Fig. S7, Table S3†). When filtered by the PCF, the turbidity of the discolored water dropped from 590 NTU to 0.53 NTU revealing that PCFs can provide effective discoloration control in the household.

4. Conclusions

PCF is commonly used as a pretreatment unit for particle removal in household water purification systems, but the controllability of various water quality risks by PCFs is still not clear. This research provides a feasible way of studying the filtration and potential risk control performance of PCFs. This is the first study to investigate the ability of the PCF in the home water purifier to intercept the particulates and DBPs in drinking water. The filtered particles concentrated on PCFs may cause toxicity to human liver cells and pose potential microbiological risks. Here, we confirmed the effectiveness of PCF in particle control, especially the outer layer (20% of the total thickness).



- 36 L. Cermakova, I. Kopecka, M. Pivokonsky, L. Pivokonska and V. Janda, *Sep. Purif. Technol.*, 2017, **173**, 330–338.
- 37 Z. Zhao, W. Sun and M. B. Ray, *Sci. Total Environ.*, 2022, **806**, 150885.
- 38 W. Li, Q. Tan, W. Zhou, J. Chen, Y. Li, F. Wang and J. Zhang, *Chemosphere*, 2020, **242**, 125310.
- 39 W. Li, F. Wang, J. Zhang, Y. Qiao, C. Xu, Y. Liu, L. Qian, W. Li and B. Dong, *Sci. Total Environ.*, 2016, **544**, 499–506.
- 40 X. Ma, G. Li, R. Chen, Y. Yu, H. Tao, G. Zhang and B. Shi, *J. Environ. Sci.*, 2020, **87**, 331–340.
- 41 X. Ma, G. Li, Y. Yu, R. Chen, Y. Zhang, H. Tao, G. Zhang and B. Shi, *Environ. Sci.: Water Res. Technol.*, 2019, **5**, 1689–1698.
- 42 I. Douterelo, K. E. Fish and J. B. Boxall, *Water Res.*, 2018, **141**, 74–85.
- 43 I. Douterelo, M. Jackson, C. Solomon and J. Boxall, *Appl. Microbiol. Biotechnol.*, 2016, **100**, 3301–3311.
- 44 H. Wang, C. R. Proctor, M. A. Edwards, M. Pryor, J. W. Santo Domingo, H. Ryu, A. K. Camper, A. Olson and A. Pruden, *Environ. Sci. Technol.*, 2014, **48**, 10624–10633.
- 45 H. Wang, M. Edwards, J. O. Falkinham and A. Pruden, *Appl. Environ. Microbiol.*, 2012, **78**, 6285–6294.
- 46 C. D. Norton, M. W. LeChevallier and J. O. Falkinham, *Water Res.*, 2004, **38**, 1457–1466.
- 47 H. Wang, C. Hu, L. Liu and X. Xing, *J. Hazard. Mater.*, 2017, **339**, 174–181.
- 48 R. Shrivastava, R. K. Upreti, S. R. Jain, K. N. Prasad, P. K. Seth and U. C. Chaturvedi, *Ecotoxicol. Environ. Saf.*, 2004, **58**, 277–283.
- 49 W. Chu, D. Yao, Y. Deng, M. Sui and N. Gao, *J. Hazard. Mater.*, 2017, **327**, 153–160.
- 50 Y. Yu, G. Li, R. Chen and B. Shi, *Water Res.*, 2021, **204**, 117582.
- 51 B. Chen, J. Jiang, X. Yang, X. Zhang and P. Westerhoff, *Water Res.*, 2021, **200**, 117265.
- 52 L. Ma, F. Peng, Q. Dong, H. Li and Z. Yang, *Chemosphere*, 2022, **296**, 133998.
- 53 Y. Zhang, Z. Lu, Z. Zhang, B. Shi, C. Hu, L. Lyu, P. Zuo, J. Metz and H. Wang, *Sep. Purif. Technol.*, 2021, **260**, 118234.

